Flow through layered vegetation in open channel flows: Effect on velocity and discharge distribution

Xiaonan Tang [1]*, Prateek K Singh [2], Yutong Guan[1], Ming Li [3]
[1] Department of Civil Engineering, Xi'an Jiaotong-Liverpool University, China
[2] Department of Building Environment and Energy Engineering, The Hongkong Polytechnic University,China
[3] Department of Civil & Environmental Engineering, The University of Liverpool, UK

Abstract

In natural river systems, layered vegetation like grass, shrubs, and tall bushes greatly affects the biodiversity, morphological process, and distribution of nutrients and pollutants. Previously, the effects of uniform one-layered vegetation on the flow structure and hydrodynamics have been extensively studied. However, due to the complexity of flow dynamics in the vegetated channel, multiple-layered vegetation has rarely been investigated. This paper presents a novel experiment to show the effect of three-layered vegetation on open channel flow. It contributes to our standing of the impact of vegetation locations and heights on the velocity and discharge distributions for a mixed vegetated channel flow. Velocities at different positions along a half cross-section were measured using a mini propeller velocimetry. Observed results showed that the velocity has a distinct profile directly behind vegetation and behind the vegetation gap. The overall trend has two specific inflections about one quarter below (0.75 z/h) or near the top of short vegetation (h): the velocity remains nearly constant in the bottom layer (z/h<0.75) and then rapidly increases until the top of short vegetation; after a gradual increase, the velocity rapidly rises to the water surface. The velocities directly behind the vegetation in the middle after short vegetation arrangement increase significantly faster than those directly behind the vegetation in the short after tall arrangement. The results showed that the maximum zonal discharge for a channel with mixed-height vegetation is situated at the mid-section of each half-channel, i.e., the area between the middle-centerline region of the near-wall regions.

This research will attain significant importance to the engineers and practitioners defining the ecological and riverine flow pattern in the presence of riparian vegetation disseminating nutrients, pollutants, and sediments.

Keywords: vegetated channel, velocity profile, submerged rigid vegetation, layered vegetation, open channel flow.

1. Introduction

The complex phenomenon of flow through vegetation array is of prime focus to better understand the physical process involved, which decisively defines the bank stability [1], pollution and nutrient transport [2], sedimentation [3], flood resistance [4, 5] and provide an ecosystem to thrive aquatics and terrestrial life [6, 7]. Macro-roughness, such as vegetation, dictates the flow resistance in rivers, wetlands, and coastal systems, considerably influencing flow structure, hydrodynamics, nutrient transmission, morphology, and biochemical processes [8-13]. Free surface flows in natural watercourses have different vegetation concerning height, density, and porosity under submerged or emergent flow conditions. During high-flow events, macrophytes, shrubs, and bushes are entirely submerged. Previously, researchers have investigated single-layered vegetation with various densities, diameters, and arrangements, exploring the flow structures and intense shearing over the edge of the submerged vegetation, depicting inflection in the vertical streamwise velocity distribution [14-17]. The flow and hydraulic resistance offered by the arrays of vegetation have also been explored simultaneously to understand the flow dynamics [18].

Furthermore, attempts have been made to model the velocity flow distribution in the emergent and submerged rigid vegetation using the mixing length hypotheses to predict and evaluate the performance of such models in different densities and configurations [19-22]. Besides the complexity of submerged and emergent single-layered vegetation, strong vertical vortices persist in the mixing zone between different vegetation heights, which are multi-mechanism overflow depths [23, 24]. Thus, vegetation interaction with flow through diverse density layers has also gained much attention by studying the flow with double-layered vegetation in laboratories [16, 25-28].

Investigating flow dynamics and resistance in the laboratory by mimicking vegetation suggests that the macro-roughness tends to act as a new layer of a river bed, which affects the bed shear through an increase in drag force as a function of surface roughness characteristics and flow depth. The concept of the new layer of roughness manifolds with the presence of vegetation array with denser on the bottom and sparser in the above, so that in a natural environment, it has different submergence with various species of vegetation. Some studies other than one submergence ratio of uniform height vegetation use the denser vegetation below and sparser above to study the dynamics of longitudinal dispersion in flow [29]. Recently, simple turbulence closure schemes were tested for submerged double-layered vegetation as drag source terms in Reynolds Averaged Navier-Stokes equations for vegetation effect [30, 31]. Furthermore, numerical simulations assisted in coping with the limitation of space, measurement, and time of experiments of flow structure in layered vegetation [32-36].

As we know, the transverse and vertical distribution of the velocity of submerged vegetation at different layers can determine zonal and overall discharge since the velocity at each flow layer varies. The velocity profile can also help in the prediction of pollutant mass transport. The channel flow with sufficient vegetation density will tend to have the highest resistance. As the flow depth increases, the sparser vegetation layer appears with the faster-moving flow. Categorically speaking, the vegetation layer can be divided into three significant levels: short being the densest, middle depicting shrubs and bushes with intermediate density, and tall with the sparsest thickness having the least resistance.

The present study aims to scrutinize the three layers of submerged vegetation mimicked by short, middle, and tall dowels at the bottom of an inclined flume, thus depicting a riparian environment in high-flow events. This paper presents a novel experimental study investigating lateral and vertical velocity change in an open channel with three-layered vegetation. Furthermore, the effect of vegetation relative to individual cross-sections is studied, identified as upstream and downstream sections of the roughness patch. This research mainly focuses on the upstream and downstream sections of the macro-roughness, where most hydrological issues occur, such as flooding, pollution dispersion, and eutrophication.

To understand the flow characteristics within the multilayered vegetated region, the present paper is arranged as follows: an experimental setting with the channel facility is described, where twelve measurement locations were chosen in two cross-sections. Then, a measuring methodology and test case conditions are elaborated. A comprehensive analysis and discussion of results are given on distributions of time-averaged streamwise velocity for all twelve locations from the side wall to the center of the channel. Then, the effect of layered vegetation at distinct locations is elaborated by comparing their averaged values in subgroups of the site, i.e., behind the vegetation and the vegetation gaps. Consequently, zonal mean velocity and discharge distribution for different layers and sub-groups of locations are shown to evaluate the impact of the vegetation from a cross-section upstream to downstream. Finally, a conclusion is drawn.

2. Experimental Setup

2.1. Flume and vegetation configuration

The experiments were conducted in a water flume at the hydraulics laboratory of Xi'an Jiaotong-Liverpool University (XJTLU). The flume is 20 m long and 0.4m wide (see Figure 1), with a fixed longitudinal bed slope $S_0 = 0.003$. A point gauge (with an accuracy of 0.1 mm) installed on a freely moveable traverse bridge is used to measure the water depth. The water depth is adjusted by the tailgate and the inflow discharge, which is also adopted by previous studies [37, 38].

The vegetation is modeled by circular plastic dowels of 6.35mm, with three different heights of 10cm, 15cm, and 20cm, representing a stem combination of various ages and heights. The vegetation zone was a combination of staggered and linear patterns of the short, middle, and tall dowels (see Figure 2). The vegetation configuration is arranged to reflect certain natural settings, consisting of denser short vegetation and sparser middle and tall vegetation, as suggested by Nepf et al. [39] and Liu et al. [16]. The distance between the adjacent dowels is 3 cm in the x and y directions.

The x, y, and z axes are selected as streamwise (positive downstream), transverse (positive towards the flume wall A), and verticle (positive upward). Under this coordinate system, x=0 indicates the flow inlet, and y=0 indicates the flume wall B, and z=0 indicates the flume bed.

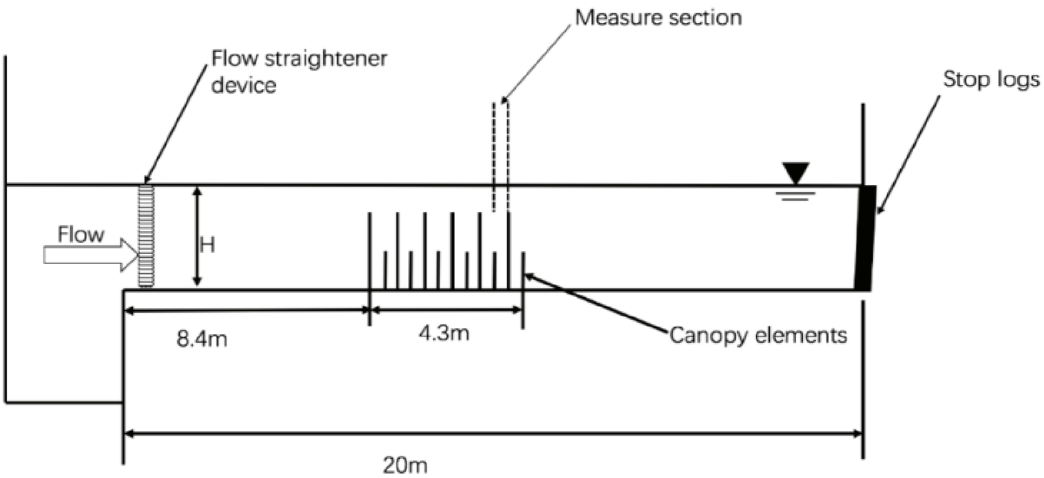

Fig.1. The schematized test flume with vegetation section (not to scale)

2.2. **Measurement methodology and flow conditions**

This experiment selected two measurement cross-sections: one upstream (x=9.65 m) and one downstream (x=10.79 m). As shown in Figure 2, the upstream cross-section is selected behind the vegetation row of short and middle dowels (10 and 15 cm), and the downstream section is selected behind the vegetation row of short and tall dowels (10 and 20 cm). The downstream cross-section is 1.14 m distant from the upstream cross-section.

For each measuring cross-section, twelve measurement locations were taken (see Figure 2). The upstream measurement locations are numbered US1, US2, to US12, where US denotes upstream. The downstream measurement locations are numbered as DS1, DS2, to DS12, where DS denotes downstream. For each measurement location, 23 vertical measurement points are measured, starting from 1 cm above the channel bed with a 1 cm interval until a measurable point close to the water surface.

The propeller velocimetry produced by Nanjing Hydraulic Research Institute was employed to measure the streamwise velocity. The working principle of the propeller is that the blade rotates as water flows, and a linear relationship exists between the rotational speed 'N' and the streamwise velocity 'u'. In this way, with the measured 'N', the streamwise velocity u can be calculated by a pre-determined linear function. This linear relationship is determined by a previous calibration test with a Norteck ADV (acoustic Doppler velocimetry). The calibration results showed that the given linear function can provide good results with an R^2 of 0.99955. In this case, we believe our measurement data is reliable. For each point, the streamwise velocity was taken as the mean value of two successive samplings, with each sampling period of 10 seconds, as suggested by the producer.

The experiments were conducted under steady flow conditions. The discharge rate Q was 27.15 L/s, and the flow depth H was 26 cm. Under this water depth, all three types of vegetation were submerged.

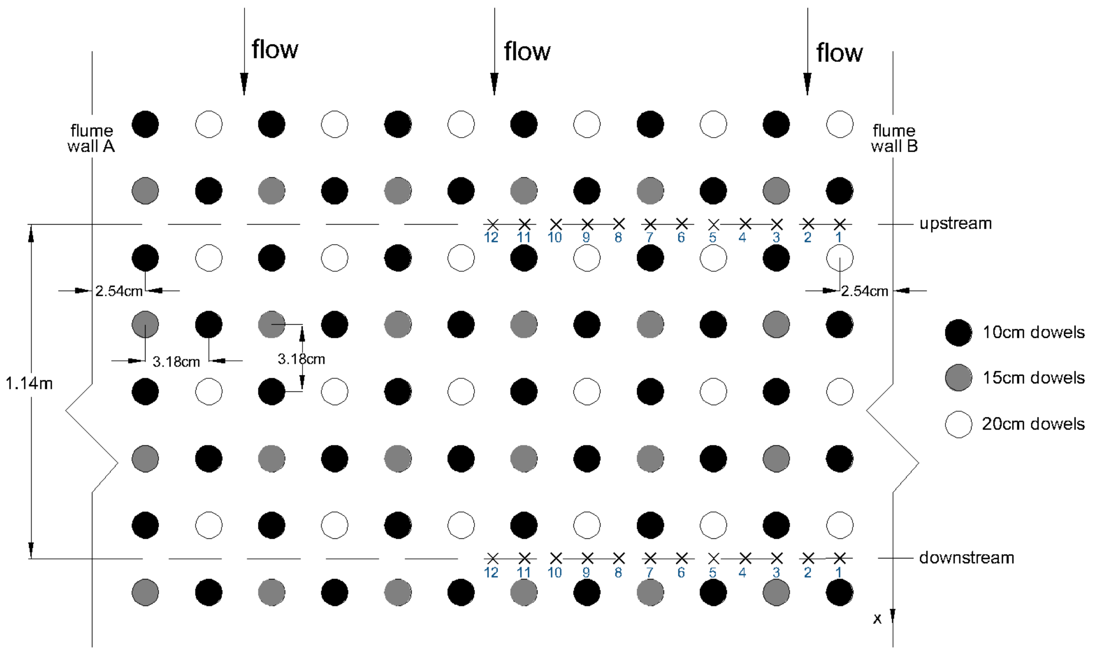

Figure 2. The vegetation configuration and measurement locations (not to scale). The black, grey, and white circles represent the short, middle, and tall dowels.

3. Results and Discussions

The normalized vertical distribution of the streamwise velocity (u/u_*) is shown in the following subsections, where u_* is the shear velocity given by Equation (1). The vertical distance (z) above the bed is normalized using the short vegetation height (h).

$$u_* = \sqrt{gHS_0} \tag{1}$$

In which g is the gravitational acceleration, taken as $9.81\ \mathrm{m}/s^2$; H is the depth of flow.

To better compare the velocity characteristics at different locations, the measurement locations are categorized into six groups based on the transverse locations: the locations behind the short-after-tall vegetation on the upstream cross-section (UST), the locations behind the middle-after-short vegetation on the upstream cross-section (UMS), the locations behind the tall-after-short vegetation on the downstream cross-section (DTS), the locations behind the short-after-middle vegetation on the downstream cross-section (DSM), the locations between the vegetation gap on the upstream cross-section (UBV), and the locations between the vegetation gap on the downstream cross-section (DBV). Herein, the initial letter of the abbreviations signifies the cross-sectional location, with 'U' denoting upstream and 'D' indicating downstream. The subsequent letters denote the vegetation arrangement, where 'S' designates short vegetation, 'M' signifies middle vegetation, 'T' represents tall vegetation and 'BV' indicates between the vegetation gap. This nomenclature scheme has been adopted to facilitate a clear and succinct delineation of the various scenarios discussed within this paper.

In addition, to compare the velocity profiles according to different column vegetation patterns, the six groups are further classified into three main groups to calculate the averaged value: the locations in the column with short-tall-short vegetation pattern (STS), the locations in the column with the short-middle-short vegetation pattern (SMS), the locations between the vegetation columns (BV). The detailed group notations and averaged value notations are summarized in Table 1.

Table 1. Detailed group notations and averaged value notations

Group Notation	Cross-sections	Locations	Combined Group Notation
UST	upstream	US1, US5, US9	STS
DTS	downstream	DS1, DS5, DS9	
UMS	upstream	US3, US7, US11	SMS
DSM	downstream	DS3, DS7, DS11	
UBV	upstream	US2, US4, US6, US8, US10, US12	BV
DBV	downstream	DS2, DS4, DS6, DS8, DS10, DS12	

3.1. **Distribution of velocity at the individual location**

This section analyzes the vertical velocity profiles at individual locations and illustrates the velocity trend of a three-layered vegetated channel flow on upstream and downstream cross-sections. Figure 3 and Figure 4 show the streamwise velocity profiles at different locations on the upstream and downstream cross-sections, respectively. These measurement locations were divided into two groups to compare the velocity profiles right behind the vegetation (location numbers 1, 3, 5, 7, 9, and 11, see Figure 3a and Figure 4a) and between the vegetation (location numbers 2, 4, 6, 8, 10, and 12, see Figure 3b and Figure 4b).

A first comparison between velocity profiles in Figure 3 and Figure 4 shows that the velocity profiles have a similar trend in different layers: In the bottom layer (layer 1), the velocity remains almost constant; in the intermediate layer (layer 2), the velocity increases gradually with a similar growth rate; in the upper layer (layer 3 and layer 4), the velocity rises rapidly until the water surface. In addition, locations 1, 5, and 9 possess a similar inter-group velocity profile, and similar inter-group profiles were also observed for locations 3, 7, 11, locations 2, 6, 10, and locations 4, 8, 12. This implies that similar vegetation patterns lead to similar vertical flow patterns.

On the upstream cross-section (see Figure 3a), the velocity curve of UST (UP1, 5, and 9) and UMS (UP3, 7, and 11) groups show different characters in layer 2 and layer 3, as the UST has one rapid velocity increase near the middle vegetation top while the UMS has two rapid velocity increase, one near the short and one near the middle vegetation top. This indicates that for UST, the flow is mainly affected by the middle dowels, while for UMS, the flow is affected by both the middle dowels and the short dowels. For the same location on the downstream cross-section (see Figure 4a), the DTS (DS1, 5, and 9) has one rapid increase near the middle dowel top and DSM (DS3, 7, and 11) has one rapid increase near the short dowel top. This indicates that for DTS, the flow is mainly affected by the middle vegetation while for DSM, the flow is mainly affected by the short vegetation. For the aforementioned velocity results, we suggest that the middle and short vegetation dominate the vertical velocity profile within the vegetation zone. The effect of tall vegetation is negligible due to its relatively lower vegetation density.

For comparative purposes, the vertical velocity structure has been divided into four layers based on vegetation height. Layer 1 encompasses the interval from the channel bottom to the top of the short vegetation. Layer 2 spans from the top of the short vegetation to the top of the middle vegetation. Layer 3 extends from the top of the middle vegetation to the top of the tall vegetation, and Layer 4 covers the space from the top of the tall vegetation to the water surface.

As shown in Figure 4b, in layer 1, the velocity profiles of DS2, DS6, and DS10 are almost identical and do not have significant variation. In layer 2, the velocity gradually increases with increasing depth, showing a position-independent profile. However, in layer 3, the velocity of DS6 is significantly greater than all the other DBV locations, which are nearly identical. This is similar to the observation of the upstream point US6 in Figure 3b, which possesses a higher velocity in layer 2 than all the other UBV locations. This indicates that the vegetation resistance in this region is less than in the other locations. All velocities are close to a single profile in the layer near the water surface. The velocity profile generally exhibits an *S*-shape with an inflection point at the edge of the vegetation top at a different level. However, the upper end of the curve may have different growth rates, depending on the position.

Within the middle vegetation layer ($z/h < 2$), the flow velocity of DS12 (in the center of the channel) is smaller than that of DS4 and DS8 (which are almost the same), implying a higher resistance in this region. The velocity gradient of DS12 becomes higher than that of DS4 and DS8 in layer 3, and their velocity difference becomes smaller above the taller vegetation. This is reasonable because the vegetation is sparser in the upper layers (layer 3 and 4), and the upper-layer flow resembles a free-flow when approaching the water surface.

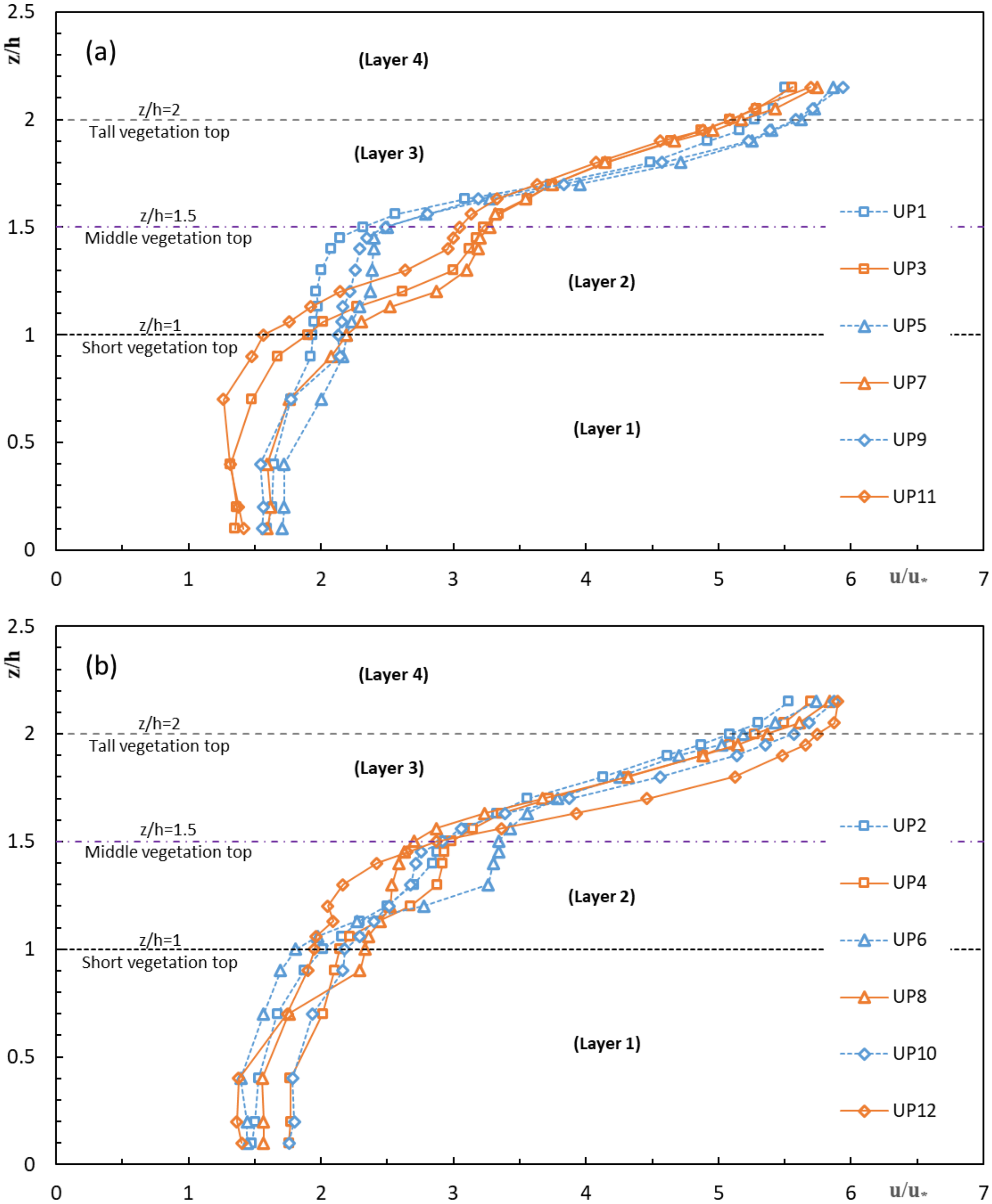

Figure 3. The vertical velocity profile on the upstream cross-section of (a) right behind the vegetation, and (b) between the vegetation

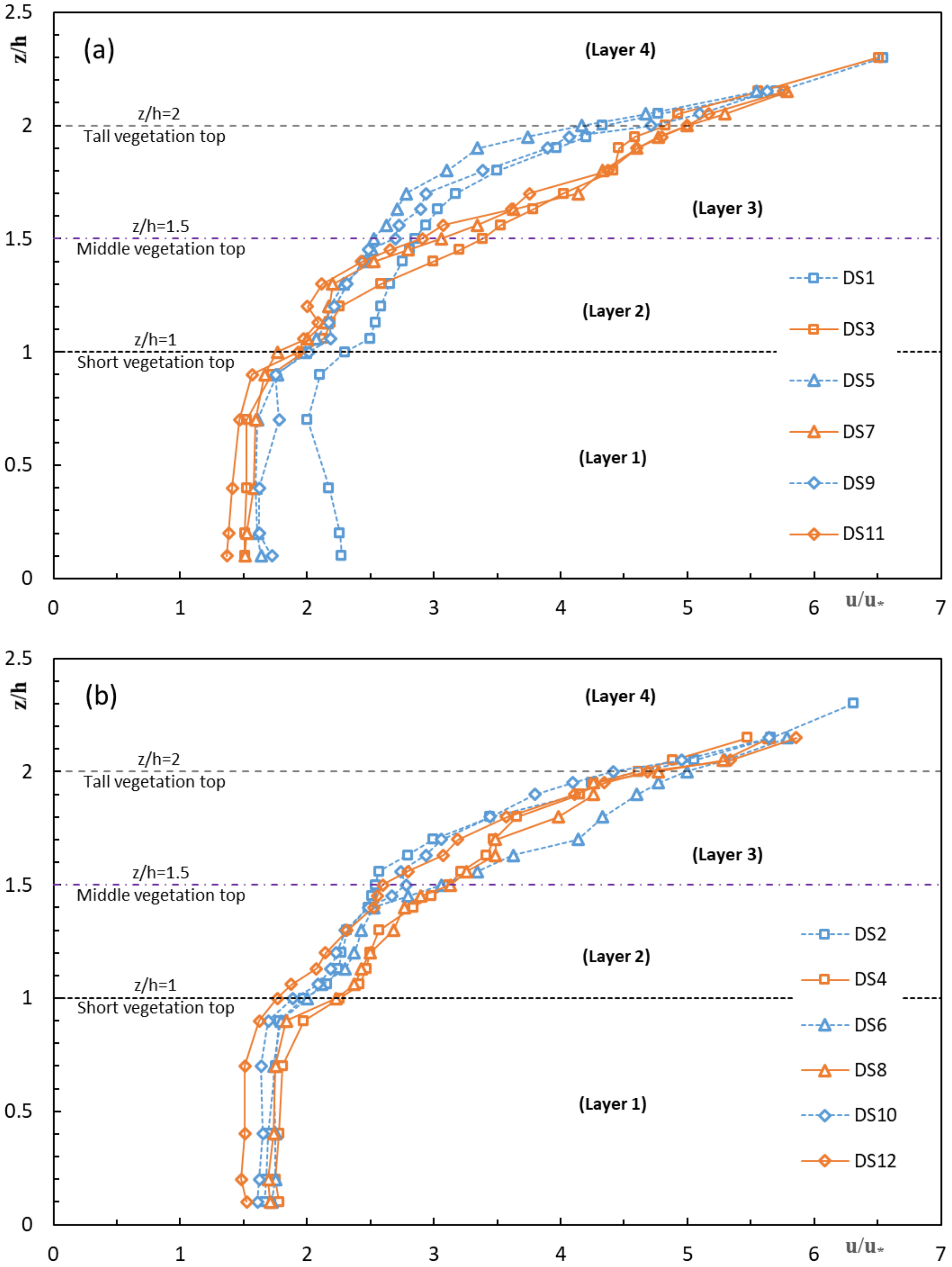

Figure 4. The vertical velocity profile on the downstream cross-section of (a) right behind the vegetation and (b) between the vegetation

In summary, vegetation has a retarding effect on the flow. The flow velocity significantly reflects near the vegetation top, while the velocity is least affected by the vegetation in the flow above the tall vegetation. In layer 1, the flow is dominated by the vegetation resistance, leading to an almost constant velocity in this layer. In layer 2 and layer 3, the flow velocity starts to increase gradually (in the densely vegetated area) and then increases rapidly (in the less densely vegetated area). In layer 4, where the free flow area, the velocity increases rapidly and reaches a stable value near the free surface.

3.2. Comparative analysis of velocities behind the vegetation at typical groups

Figure 5a and 5b demonstrates the averaged vertical velocity profiles of locations with similar geometry patterns in this region, which covers UST upstream, DTS downstream, and their cross-sectional averaged STS. Figure 6a illustrates the vertical velocity profiles of upstream UMS and downstream DSM, and Figure 6b helps to understand the averaged character of the upstream and downstream cross-sections.

As shown in Figure 5, the overall mean velocity profile of UST has an inflection point at 1.5 z/h, howing the significant shedding effect of middle upstream vegetation on the velocity in the lower layer. For the downstream DTS, the inflection point is a little higher than the upstream UST, near z/h=1.7. This implies that the overall vegetation drags at the downstream DTS decrease at a higher position than that at the upstream UST. In addition, the velocity of downstream DTS in layer 2 is greater than that of upstream UST at the same height in layer 2, while the velocity of downstream DTS in layer 3 is smaller than that of upstream UST at the same height in layer 3. This implies that the vegetation resistance of upstream UST is higher than DTS in layer 2, while the vegetation resistance of downstream DTS is higher than UST in layer 3. As the only difference between upstream UST and downstream DTS is the measurement location, we suggest that for the same vegetation pattern, the location behind the middle vegetation possesses a higher drag force in layers above the middle vegetation top than that in the locations behind the short vegetation and that the vertical influenced zone of the vegetation resistance is higher for the locations behind the tall vegetation.

The overall averaged velocity profile is a S-shaped type (see Figure 5b), i.e., the velocity changes small in the bottom region up to $0.9h$ and then increases quickly near the top of short vegetation (i.e., $z/h = 1$), where the strong vertical momentum exchange occurs. The velocity gradually increases in the intermediate region ($1 < z/h < 1.5$) and starts rising sharply until the water surface.

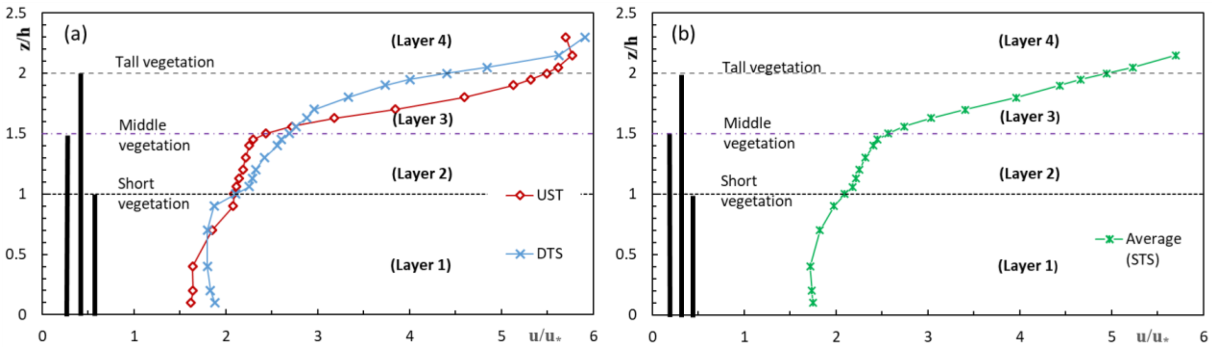

Figure 5. The velocity distribution at (a) upstream behind short-after-tall vegetation (UST) and downstream behind tall-after-short vegetation (DTS); and (b) the average of the velocity at both sections.

As shown in Figure 6a, the vertical profiles of the upstream UMS and downstream DSM is almost the same unless in layer 2 ($1 < z/h < 1.5$), where the velocity at UMS is bigger than that at DSM. This implies that in the layer 2, for the SMS vegetation pattern, the overall resistance at locations behind the middle vegetation is higher than that at locations behind the short vegetation.

When comparing the averaged vertical velocity profiles of group STS and group SMS (see Figure 5b and Figure 6b), it is evident that the velocity of STS is bigger than that of SMS in layer 1, but the velocity of SMS is accelerating faster than that of STS in layer 2. In layer 3 and layer 4, the velocity gradient of both STS and SMS remains constant, indicating negligible vegetation resistance in these layers, which is consistent with the previous findings. In addition, the inflection point of STS occurs near the middle vegetation topo, while the inflection point of SMS occurs near the short vegetation top. This implies that vegetation drag dominates the flow of layer 1 and layer 2 for STS locations while only dominate the flow of layer 1 for SMS locations.

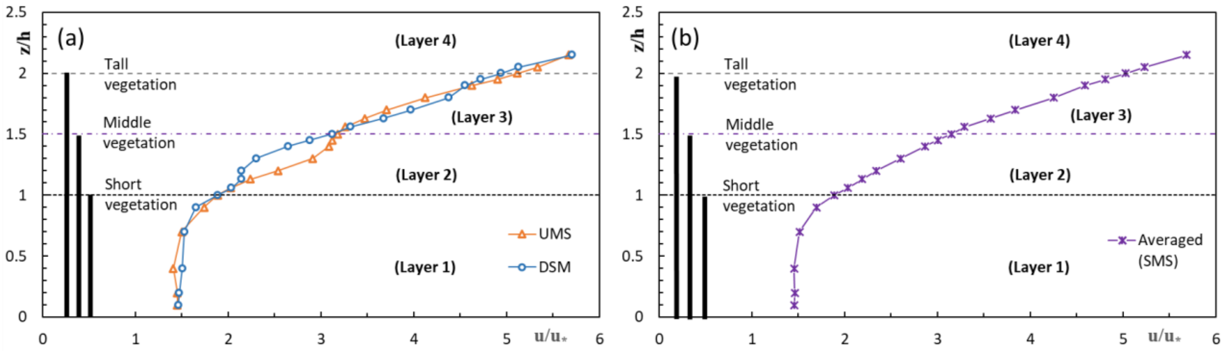

Figure 6. The velocity distribution at (a) upstream behind the middle-after-short vegetation (UMS) and downstream behind the short-after-middle vegetation (DSM) and (b) the average of the velocity at both sections.

3.3. Comparative analysis of velocities between gaps of the vegetation

In this section, we mainly focus on the velocity profiles of UBV and DBV locations. The influence on the velocity distribution at the gap of short and middle (UBV) and short and large (DBV) is depicted in Figure 7a, to compare the velocity variation on these two cross-sections. The averaged value of upstream UBV and downstream DBV is shown in Figure 7b to reflect the general velocity profile of locations between vegetation gaps.

In Figure 7a, the inflection point in the trend upstream behind the gap of short and middle vegetation (UBV) is significant at the upper layer 1, $z/h < 1$ and layer 2, $z/h = 1.5$. In the upstream cross-sectional area, middle-height vegetation predominantly impacts layers 2, 3, and 4. The averaged value of the velocity on upstream and downstream cross-sections in Figure 7b subsides the effect of the flow gradient at the $z/h = 1$ and 1.5, which is much more pronounced, otherwise in the individual distribution at the upstream and downstream cross-section.

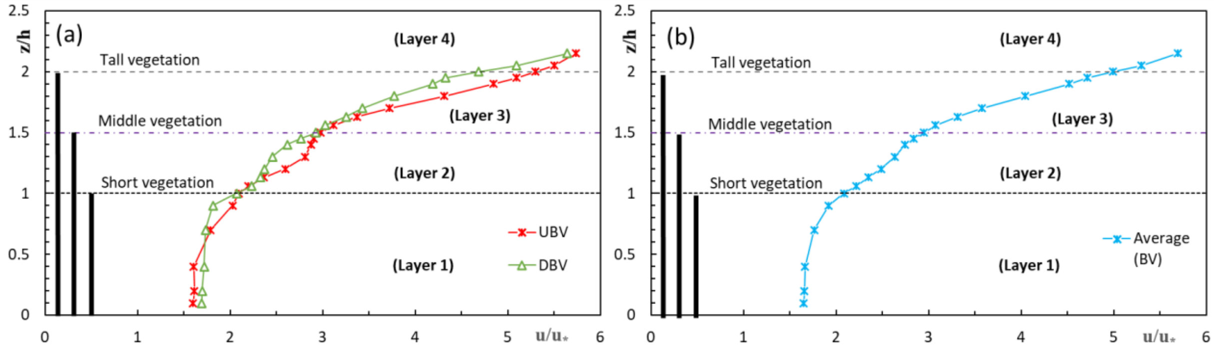

Figure 7. The velocity distribution at (a) upstream behind the gap between short and middle vegetation (UBV) and downstream behind the gap between short and tall vegetation (DBV) and (b) the average of the velocity at both sections.

3.4. Impact of vegetation height on group locations

This section focuses on the comparison of velocity profiles among different groups, with each group covering locations of similar vegetation patterns. Figure 8 shows the group-averaged velocity profiles, following the group method described in Table 1. For the purpose to compare the velocity profile between each group and the whole channel flow, we introduced a channel-averaged velocity profile (UD), which is the averaged value of the velocities at the same z-value across both upstream and downstream cross-sections.

In the lower layer (layer 1), the velocities of UST, DTS, UMS, DSM, UBV, and DBV exhibit minimal variation. They remain relatively constant from the bed up to approximately 0.75 z/h, after which a gradual acceleration in velocity is observed. It is important to note, however, that this description offers a broad overview of the velocity distribution in the presence of a bluff body within an open channel flow. A more nuanced understanding of how different combinations of vegetation height impact this distribution is provided in this section, as further illustrated in Figure 8a and 8b.

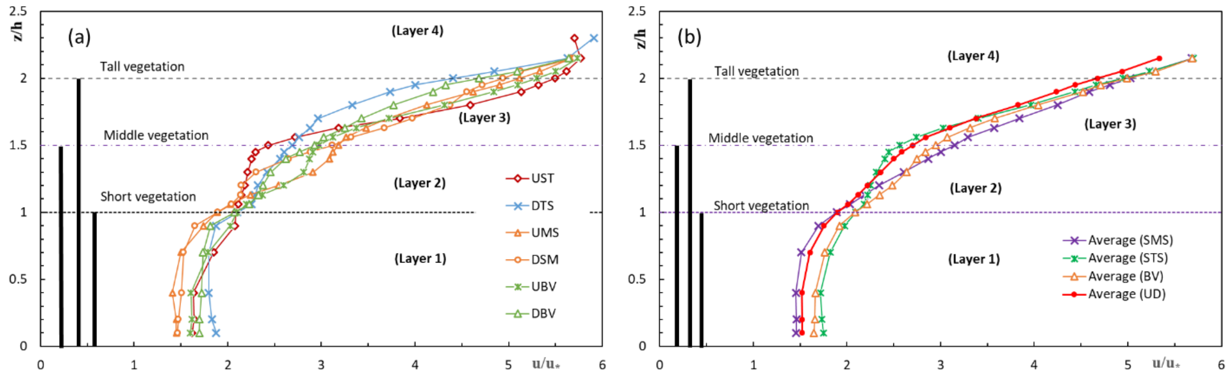

Figure 8. (a) The average velocity distribution at the typical locations over upstream and downstream sections; (b) the average of all sites of two sections.

It was found that when $z/h < 1.3$, the flow velocity of UMS and DSM is smaller than that of UST, DTS, UBV, and DBV. Nevertheless, when $z/h > 1.3$, the flow velocity change of UMS and DSM is faster and more prominent than that of DTS and DBV. The velocity profiles of all groups tend to reach the same maximum velocity in layer 4. It is an interesting observation that for UST group, the velocity in layer 4 has a turning point, where the velocity is decelerating and then re-accelerating to the its highest value near the water surface. This implies that for an STS column vegetation pattern, the locations behind the short dowels are still affected by the tall vegetation above the tall vegetation top (layer 4). In general, the velocity of UST and DTS is lower than those of other sites in layer 2, indicating that the more layered the vegetation, the slower the velocity.

In the upper layer (layers 3 and 4), the velocities of all groups (except DTS) have an apparent gradient of velocity at the top of the middle vegetation (i.e., $z/h = 1.5$) and then increase rapidly towards the water surface. As expected in this layer, the additional resistance caused by vegetation is limited and has little impact at this depth where only tall vegetation is present (i.e., the most scattered layer). It is noted that the velocity of UST is higher, which may be due to the edge effect of tall vegetation. On the contrary, DTS is the least among all the positions in the layer between $1.5 \leq z/h \leq 2.0$.

Figure 8b is an overall (averaged) velocity profile for three specific positions. Based on the averaged velocity profile (UD), the overall velocity in this three-layered vegetated channel remains almost constant in the bottom layer ($z/h < 0.75$), increases fast to the top of short vegetation (z/h=1), and then increases gradually to the middle of layer 2 ($1 < z/h < 1.5$); afterward, it increases fast until the water surface in the upper layer ($z/h > 1.5$). Compared to single-layered vegetation, in multilayered vegetation, the velocity inflection is significantly associated with the top edge of different-height vegetation (i.e., the sudden change of vegetation density). In addition, for practical applications where high precision is not a stringent requirement, the velocity profile of the UD group can serve as a reasonable approximation for the velocity profiles at various locations within the channel. Generally, in layer 1, the differences between UD and SMS are minimal, and notably smaller than those between BV and STS. In layers 2, 3, and 4, the velocity profiles of UD and STS exhibit closer similarities, being notably smaller than those of BV and SMS. Thus, the implementation for sediment, nutrient, and pollutant transport will be significantly addressed by the velocity distribution depicted by the UD with the consecutive point of inflection suggested by the multilayered vegetation. Moreover, the averaged velocity profile for multilayered vegetation needs an analytical solution for eddy viscosity at $z/h \approx 0.75 \,\&\, 1.5$, like one-layered vegetation having inflection over the top edge of the vegetation.

3.5. Distributions of zonal-averaged velocity and discharge

It is important to determine the zonal velocity and zonal discharge distributions in different layers for engineering use. This section explores how the zonal velocity and discharge change along the flume. The zonal velocity and layer velocity are normalized by the mean cross-sectional velocity U (given by $U = Q/A$, where Q is the flow discharge and A is the area of the measuring cross-section), and the half channel is split into three zones: Zone 1-4, 4-8, and 8-12. Herein, Zone 1-4 is the region from location number 1 to location 4; Zone 4-8 is the region from location number 4 to location 8; Zone 8-12 is the region from location number 8 to location 12.

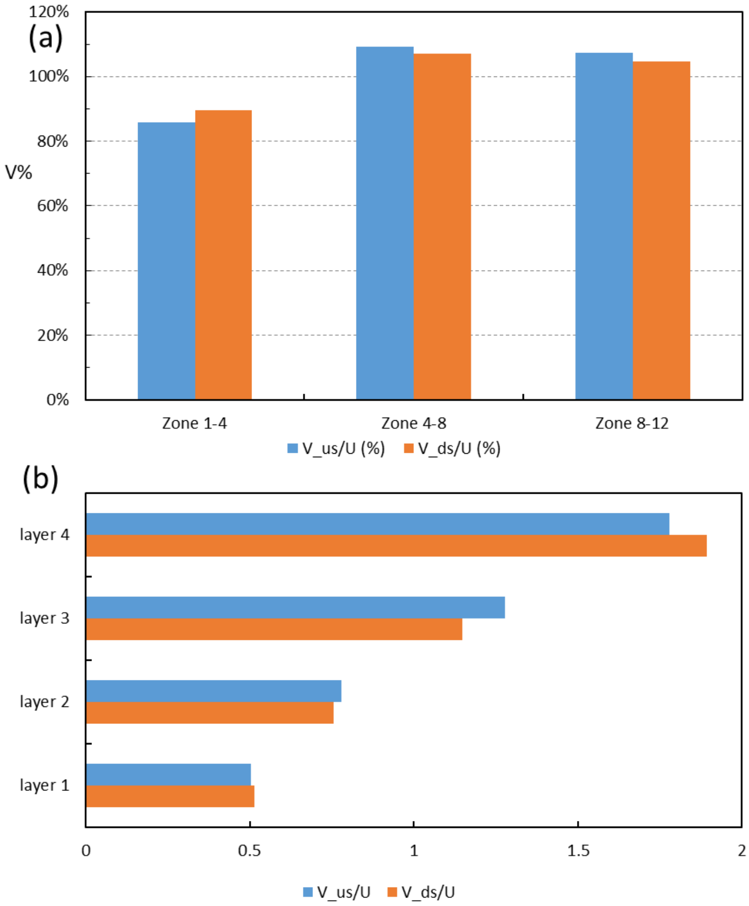

Figure 9. The upstream and the downstream distributions of (a) zonal-averaged velocity and (b) layer-averaged velocity (V), where the subscript us denotes upstream and the subscript ds denotes downstream.

Figure 9a illustrates the corresponding zonal-averaged velocity distributions for Zone 1-4, Zone 4-8, and Zone 8-12. The zonal velocity in the region closer to the wall (Zone 1-4) is about 10-15% smaller than that in Zone 4-8 and Zone 8-12. Interestingly, the zonal velocity around the centerline region of the channel (i.e., Zone 8-12) is not the highest among the three zones. Instead, Zone 4-8 possesses the highest zonal-averaged velocity in both upstream and downstream cross-sections, indicating that the vegetation resistance in Zone 8-12 is a little higher than that in Zone 4-8. Figure 9b shows that the layer-averaged velocity increases with increasing flow depth, as the highest velocity was found in the top layer (layer 4) while the lowest velocity was near the bed (layer 1). The highest layer-averaged velocity occurs near the free surface, which is consistent with the previous results of vertical velocity profiles.

It is also worth noting that the downstream layer-averaged velocity in layer 4 is higher than that of the upstream cross-section. This implies that compared to SMS, the STS vegetation pattern will result in a higher layer-averaged velocity in the free-flow region above all the vegetation. In addition, the layer-averaged velocity of upstream SMS pattern in layer 2 and layer 3 is smaller than that of downstream STS pattern. In layer 1, the layer-averaged velocity is almost the same for both cross-sections and the smallest layer-averaged velocity is observed in this layer, indicating a maximum vegetation resistance occurs here.

Based on the zonal-averaged velocity distributions (see Figure 9), the upstream and downstream zonal discharge of the half channel is computed (see Figure 10). Figure 10a shows that upstream discharge in the zone closer to the wall (Zone 1-4) is about 2% smaller than in Zone 4-8 or Zone 8-12. Similarly, downstream Zone 1-4 has the smallest discharge, with a difference of less than 1% compared to downstream Zone 4-8 and downstream Zone 8-12 (see Figure 10b). Zone 4-8 has the highest zonal discharge on both cross-sections, being 17.01% of the upstream section and 17.33% of the downstream section.

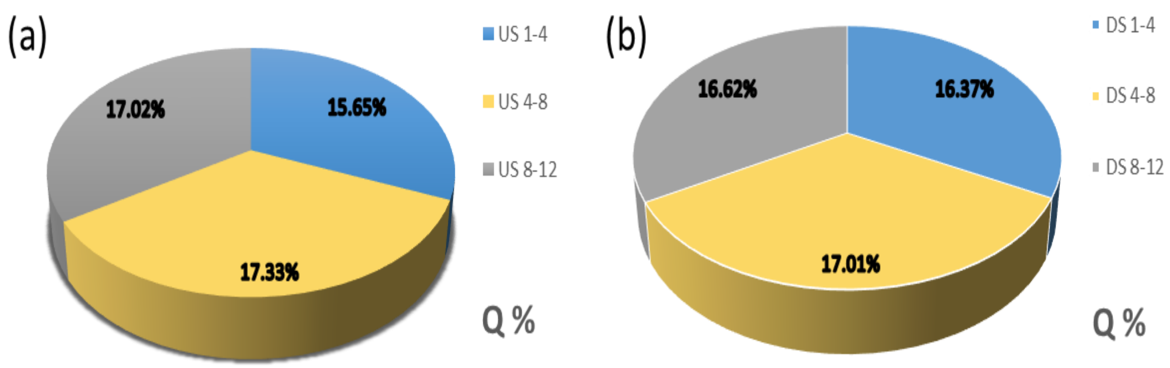

Figure 10. Percentage of zonal discharge at (a) upstream; (b) downstream.

4. Conclusions

A novel experiment was designed and conducted to explore the impact of mixed height vegetation on flow structure. The vertical velocity profiles are analyzed according to different locations (zones) and different positions (layers). Generally speaking, the velocity is almost constant in the lower layer ($z/h < 0.5$), increasing rapidly up to the short vegetation top and then continuously increasing to the water surface. The velocity profile shows two distinct inflections: one near $z/h = 0.75$, the other near the top of short vegetation. It is evident from the results that the velocity profile is different for the directly behind short-after-tall vegetation (UST) and directly behind tall-after-short vegetation (DTS) in layer 3. The main findings are shown below.

- The flow is mainly affected by the short and middle vegetation, and the effect of tall vegetation is negligible. The flow velocity above the middle vegetation top increases rapidly until the water surface, and the velocity gradient in this layer is almost constant.

- The velocity profiles directly behind vegetation are affected by the vegetation pattern: For an STS line pattern, the velocity increases slowly with the water depth when behind tall vegetation in the upper layer ($z/h>1$), but it increases rapidly to the water surface when behind short vegetation. For an SMS line pattern, the velocity increases slowly with the water depth when behind short vegetation in layer 2 ($1 < z/h < 1.5$), but it creases rapidly to the water surface when behind middle vegetation.

- For a channel with mixed height vegetation, the maximum zonal discharge occurs in the zone between the middle centerline region and the near wall region (i.e., Zone 4-8).

In the future, the study can be investigated on the turbulent structure of the mixed layered-vegetation channel flow. Also, understanding the flow structures in the three vegetation zones with distinct densities will help us understand the physical behavior of flow through layered or non-uniformly distributed vegetation in the riverine ecosystem.

Acknowledgement

The authors would like to acknowledge the support from the National Natural Science Foundation of China (11772270) and the research funding of XJTLU (REF-20-02-03 and PGRS2012007).

Credit authorship contribution statement

X. Tang: Conceptualization, Methodology, Supervision, Data analysis, Editing and Review, Funding acquisition; **P. Singh:** Analysis, Writing – original draft; **Y. Guan:** Analysis, Writing – review & editing ; **M. Li:** Review

Data Availability

The corresponding author will avail the data on reasonable request.

Declaration of Competing Interest

The authors declare that they have no known competing financial interests or personal relationships that could have influenced the work reported in this paper.

References

1. Abernethy, B. and I.D. Rutherfurd, *The distribution and strength of riparian tree roots in relation to riverbank reinforcement.* Hydrological processes, 2001. **15**(1): p. 63-79.
2. Scheumann, W., I. Sagsen, and E. Tereci, *Orontes River Basin: Downstream challenges and prospects for cooperation.* Turkey's Water Policy: National Frameworks and International Cooperation, 2011: p. 301-312.
3. Armanini, A. and V. Cavedon, *Bed-load through emergent vegetation.* Advances in Water Resources, 2019. **129**: p. 250-259.
4. Box, W., J. Järvelä, and K. Västilä, *Flow resistance of floodplain vegetation mixtures for modelling river flows.* Journal of Hydrology, 2021. **601**: p. 126593.
5. Shi, H., X. Liang, W. Huai, and Y. Wang, *Predicting the bulk average velocity of open-channel flow with submerged rigid vegetation.* Journal of Hydrology, 2019. **572**: p. 213-225.
6. Rowiński, P.M., K. Västilä, J. Aberle, J. Järvelä, and M.B. Kalinowska, *How vegetation can aid in coping with river management challenges: A brief review.* Ecohydrology & Hydrobiology, 2018. **18**(4): p. 345-354.
7. Naiman, R.J., H. Decamps, and M. Pollock, *The role of riparian corridors in maintaining regional biodiversity.* Ecological applications, 1993. **3**(2): p. 209-212.
8. Wang, C., S.-s. Zheng, P.-f. Wang, and J. Hou, *Interactions between vegetation, water flow and sediment transport: A review.* Journal of Hydrodynamics, 2015. **27**(1): p. 24-37.
9. Nepf, H.M., *Flow and transport in regions with aquatic vegetation.* Annual review of fluid mechanics, 2012. **44**: p. 123-142.
10. Tang, C., Y. Yi, and S. Zhang, *Flow and turbulence in unevenly obstructed channels with rigid and flexible vegetation.* Journal of Environmental Management, 2023. **326**: p. 116736.

11. Nezu, I. and M. Sanjou, *Turburence structure and coherent motion in vegetated canopy open-channel flows.* Journal of hydro-environment research, 2008. **2**(2): p. 62-90.
12. Ghisalberti, M. and H.M. Nepf, *Mixing layers and coherent structures in vegetated aquatic flows.* Journal of Geophysical Research: Oceans, 2002. **107**(C2): p. 3-1-3-11.
13. Caroppi, G., P. Gualtieri, N. Fontana, and M. Giugni, *Effects of vegetation density on shear layer in partly vegetated channels.* Journal of Hydro-Environment Research, 2020. **30**: p. 82-90.
14. Raupach, M.R., J.J. Finnigan, and Y. Brunet, *Coherent eddies and turbulence in vegetation canopies: the mixing-layer analogy.* Boundary-Layer Meteorology 25th Anniversary Volume, 1970–1995: Invited Reviews and Selected Contributions to Recognise Ted Munn's Contribution as Editor over the Past 25 Years, 1996: p. 351-382.
15. Liu, D., P. Diplas, J. Fairbanks, and C. Hodges, *An experimental study of flow through rigid vegetation.* Journal of Geophysical Research: Earth Surface, 2008. **113**(F4).
16. Liu, D., P. Diplas, C. Hodges, and J. Fairbanks, *Hydrodynamics of flow through double layer rigid vegetation.* Geomorphology, 2010. **116**(3-4): p. 286-296.
17. Guan, Y., X. Tang, and Y. Zhang. *The Impact of Double-layered Rigid Vegetation on Flow Structure*. in *Proceedings of the 9th International Symposium on Environmental Hydraulics*. 2021. Seoul National University, Seoul, Korea.
18. Stone, B.M. and H.T. Shen, *Hydraulic resistance of flow in channels with cylindrical roughness.* Journal of hydraulic engineering, 2002. **128**(5): p. 500-506.
19. Tang, X., *An improved analytical model for vertical velocity distribution of vegetated channel flows.* Journal of Geoscience and Environment Protection, 2019. **7**(04): p. 42-60.
20. Tang, X., *A mixing‐length‐scale‐based analytical model for predicting velocity profiles of open‐channel flows with submerged rigid vegetation.* Water and Environment Journal, 2019. **33**(4): p. 610-619.
21. Wang, Z., H. Zhang, X. He, Q. Jiang, W. Xu, and W. Tian, *Effects of vegetation height and relative submergence for rigid submerged vegetation on flow structure in open channel.* Earth Sciences Research Journal, 2022. **26**(1): p. 39-46.
22. Singh, P., H. Rahimi, and X. Tang, *Parameterization of the modeling variables in velocity analytical solutions of open-channel flows with double-layered vegetation.* Environmental Fluid Mechanics, 2019. **19**(3): p. 765-784.
23. Nikora, N., V. Nikora, and T. O'Donoghue, *Velocity profiles in vegetated open-channel flows: combined effects of multiple mechanisms.* Journal of Hydraulic Engineering, 2013. **139**(10): p. 1021-1032.
24. Kumar, P. and A. Sharma, *Experimental investigation of 3D flow properties around emergent rigid vegetation.* Ecohydrology, 2022. **15**(8): p. e2474.
25. Tang, X., H. Rahimi, P. Singh, S. Yuan, and C. Lu, *Analytical Modeling of Mean Velocity Profile through Two-Layered Fully Submerged Vegetation.* Journal of Hydraulic Engineering, 2023. **149**(2): p. 04022041.
26. Tang, X., H. Rahimi, Y. Guan, and Y. Wang, *Hydraulic characteristics of open-channel flow with partially-placed double layer rigid vegetation.* Environmental Fluid Mechanics, 2021. **21**: p. 317-342.
27. Rahimi, H., X. Tang, P. Singh, M. Li, and S. Alaghmand, *Analytical model for the vertical velocity profiles in open channel flows with two layered vegetation.* Advances in Water Resources, 2020. **137**(3): p. 103527.
28. Huai, W., W. Wang, Y. Hu, Y. Zeng, and Z. Yang, *Analytical model of the mean velocity distribution in an open channel with double-layered rigid vegetation.* Advances in Water Resources, 2014. **69**: p. 106-113.
29. Lightbody, A. and H. Nepf, *Prediction of near-field shear dispersion in an emergent canopy with heterogeneous morphology.* Environmental Fluid Mechanics, 2006. **6**: p. 477-488.

30. Souliotis, D. and P. Prinos, *Effect of a vegetation patch on turbulent channel flow.* Journal of Hydraulic Research, 2011. **49**(2): p. 157-167.
31. Neary, V., *Numerical solution of fully developed flow with vegetative resistance.* Journal of engineering mechanics, 2003. **129**(5): p. 558-563.
32. Marjoribanks, T.I., R.J. Hardy, S.N. Lane, and D.R. Parsons, *Does the canopy mixing layer model apply to highly flexible aquatic vegetation? Insights from numerical modelling.* Environmental Fluid Mechanics, 2017. **17**: p. 277-301.
33. Anjum, N. and M. Ali, *Investigation of the flow structures through heterogeneous vegetation of varying patch configurations in an open channel.* Environmental Fluid Mechanics, 2022: p. 1-22.
34. Rahimi, H., X. Tang, and P. Singh, *Experimental and numerical study on impact of double layer vegetation in open channel flows.* Journal of Hydrologic Engineering, 2020. **25**(2): p. 04019064.
35. Ghani, U., N. Anjum, G.A. Pasha, and M. Ahmad, *Numerical investigation of the flow characteristics through discontinuous and layered vegetation patches of finite width in an open channel.* Environmental Fluid Mechanics, 2019. **19**(6): p. 1469-1495.
36. Tang, X., S. Zhang, J. Cao, H. Wang, N. Xiao, and Y. Guan. *Effect of Multiple Layered Vegetation on the Velocity Distribution of Flow in an Open Channel*. in *Proceedings of the 39th IAHR World Congress*. 2022. IAHR.
37. Liu, C., Y. Shan, W. Sun, C. Yan, and K. Yang, *An open channel with an emergent vegetation patch: Predicting the longitudinal profiles of velocities based on exponential decay.* Journal of Hydrology, 2020. **582**: p. 124429.
38. Caroppi, G., K. Västilä, P. Gualtieri, J. Järvelä, M. Giugni, and P.M. Rowiński, *Comparison of flexible and rigid vegetation induced shear layers in partly vegetated channels.* Water Resources Research, 2021. **57**(3): p. e2020WR028243.
39. Nepf, H., B. White, A. Lightbody, and M. Ghisalberti. *Transport in aquatic canopies*. in *Flow and Transport Processes With Complex Obstructions: Applications to Cities, Vegetative Canopies, and Industry*. 2007. Springer.
40. Van Prooijen, B.C., J.A. Battjes, and W.S. Uijttewaal, *Momentum exchange in straight uniform compound channel flow.* Journal of hydraulic engineering, 2005. **131**(3): p. 175-183.